Upgrade of the 15 T JUMBO Facility for Time Dependent High Resolution $U(I)$-Measurements

Frank Hornung and Theo Schneider

***Abstract*—The detailed knowledge of the voltage-current characteristics $U(I)$ of a superconductor and therefore its critical current I_C and n-value is a prerequisite for the application of these materials. In the past, we focussed on the high resolution $U(I)$-determination under quasi steady-state conditions in order to avoid transient voltage contributions and to average out noise in $U(I)$. The drawback of this measuring technique is that possible additional effects occurring during the variation of the current such as flux flow instabilities are, in principle, not detected. Therefore, the facility JUMBO was upgraded to allow also continuous high resolution measurements of $U(I)$ while ramping the current. In addition to the advancement of the measuring equipment, grounding and shielding of the whole facility was improved to reduce the influence of electromagnetic perturbations. In this paper, first measurement results with this new setup are presented and the impact of the current-ramping on the $U(I)$-measurements is discussed.**

***Index Terms*—Continuous measurement, critical current, n-value, voltage-current characteristics.**

I. Introduction

THE workhorse for everyday $U(I)$-measurements of superconductors in external magnetic fields in the High Field Laboratory of the Institute for Technical Physics is the facility JUMBO. Its basic superconducting magnet configurations produce a field of up to 15 T in a bore of 44 mm and 10 T in 100 mm at a helium bath temperature of 4.2 K. Further details about the facility are described in [1].

In the past we focused on the $U(I)$-determination in the so-called 'step-and-hold'-technique. After a discrete current step there is a delay of several seconds before measurement of the voltage under quasi steady-state conditions in a resistive four-point configuration [2]. The advantage of this method is the high resolution due to avoiding transient contributions to the signal and the averaging out of noise. With this technique numerous low- and high-temperature superconductors were characterized in the past ([3]–[9]) to develop superconducting high-field magnets for research facilities and nuclear magnetic resonance (NMR) spectrometers [1].

The drawback of the 'step-and-hold' measuring technique is that it is very time consuming and that possible transient effects occurring during the variation of the current are, in principle, not detected. Therefore, to speed up the measurement time and to gain access to transient effects, JUMBO was upgraded for continuous high resolution measurements of $U(I)$ while ramping the current.

The authors are with the Forschungszentrum Karlsruhe, Institute for Technical Physics, Hermann-von-Helmholtz-Platz 1, 76344 Eggenstein-Leopoldshafen, Germany (e-mail: frank.hornung@itp.fzk.de, http://www.fzk.de/itp; theo.schneider@itp.fzk.de).

II. Upgrade of the 15 T Jumbo Facility

When performing ramped $U(I)$-measurements it is essential to minimize transient voltage contributions that are not caused by the sample, but by the experimental facility. To achieve this goal, grounding, potential equalization, and shielding of the different components of the JUMBO facility (cryostat, power supplies, control systems, measuring equipment, etc. [1], [2]) were revised to eliminate ground loops and to reduce the influence of electromagnetic perturbations. Furthermore, all measuring equipment is now powered by separate isolating transformers.

A new analog ramp generator with excellent ramp rate stability was constructed to drive the DC power supply for the sample current. While ramping the current, the voltage drop along two measuring lengths $L_{1,2}$ of the sample is detected by means of two nano-voltmeters. For the determination of the current a third digital voltmeter measures the voltage drop across a shunt-resistor. The triggered data acquisition is computer-controlled. All voltmeters are readout by their GPIB interfaces. With this setup a sampling rate of 14 Hz is achieved with a typical resolution of $\pm 1 \times 10^{-9}$ V/cm ($L \approx 100$ cm).

III. Ramped High Resolution $U(I)$-Measurements

A. Contributions to the Measured Voltage

For investigation of the detected voltage U in a ramped high resolution $U(I)$-measurement, the areas $A_{1,2}$, which are spanned by the measuring lengths $L_{1,2}$ of the superconductor and the voltages taps soldered to the sample connecting the superconductor with the voltmeters, have to be considered. Even in the case of twisted pairs of voltage-taps and the co-winding of one of the voltage-taps of each pair along the measuring length, the enclosed areas $A_{1,2}$ are non-zero as illustrated in Fig. 1.

In principle, the measured voltage $U(I)$ can be partitioned into three parts: The voltage caused by the superconducting transition, U_{SCT}, the inductive voltage, U_{IND}, caused by the time variation of the flux $\phi_{1,2}$ through the areas $A_{1,2}$, $-\mathrm{d}\phi_{1,2}/\mathrm{d}t$, and the sum of all other potential contributions U_{other}:

$$U(I) = U_{\mathrm{SCT}} + U_{\mathrm{IND}} + U_{\mathrm{other}}. \tag{1}$$

B. Contributions to U_{IND}

The flux $\phi_{1,2}$ is given by $\int B \, \mathrm{d}A_{1,2}$. There are three causes that may alter $\phi_{1,2}$: Variation of the external background field

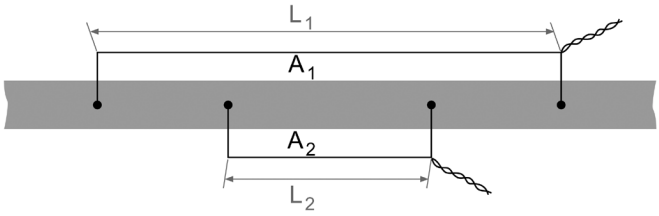

Fig. 1. Schematic diagram of the detection of the voltage along two measuring lengths $L_{1,2}$ of a superconducting wire. Even in the case of twisted pairs of voltage-taps and the co-winding of one of the voltage-taps of each pair along the measuring length, the enclosed areas $A_{1,2}$ are non-zero.

B_{ex}, variation of the external self-field $B_{\mathrm{sf,ex}}$ produced by the specimen in its surrounding volume, and the variation of the enclosed areas $A_{1,2}$.

Regarding the investigated samples, the superconducting wire and the voltage-taps were pasted over with Stycast. The enclosed areas $A_{1,2}$ therefore did not vary during the entire measurement. This fact was confirmed by $U(I)$-measurements with parallel and antiparallel orientation of the background field and the self-field of the coils. Despite the different Lorentz-force acting on the wire in the two cases there was no changing contribution.

As the measurements were performed in different but constant external fields B_{ex}, no contribution to U_{IND} is generated by B_{ex} neither.

Due to the ramping of the current $I(t)$ the external self-field $B_{\mathrm{sf,ex}}(t)$ produced by the sample is changed. The experiments were performed with constant ramp rates $\mathrm{d}I/\mathrm{d}t$. As $B_{\mathrm{sf,ex}}(t)$ is proportional to $I(t)$, the ramping leads to constant offset voltage contributions.

C. Contributions to U_{other}

Twisting of composite superconductors is ineffective with regard to the self-field produced by the transport current. The filaments are coupled and the composite behaves to a good approximation like a untwisted or bulk superconductor [10], [11]. Therefore, when increasing the transport current $I(t)$ the self-field enters the superconductor starting at the surface. The superconducting current is restricted to the penetrated area and flows with the engineering current density j_{e} as the average current density over filaments and matrix. The penetrated area $A_p(t)$ is given by: $j_{\mathrm{e}} \times A_p(t) = I(t)$.

For a wire with cylindrical geometry with radius a which is in the critical state in the interval $[r_{\mathrm{sat}}, a]$ the variation of the azimuthal field $B_\varphi(r)$ within the composite is given by

$$B_\varphi(r) = \frac{\mu_0 I(t)}{2\pi r} - \frac{\mu_0 j_{\mathrm{e}}}{2r}(a^2 - r^2) \quad \text{for } r_{\mathrm{sat}} < r < a. \tag{2}$$

Using Faraday's law in cylindrical coordinates one obtains for the electrical field $E_z(r)$ with the assumed approximation:

$$E_z(r) = \frac{\mu_0}{2\pi}\frac{\mathrm{d}I}{\mathrm{d}t}\ln\frac{r}{r_{\mathrm{sat}}}. \tag{3}$$

In a measurement, the electrical field $E = U/L$ on the surface of the wire is detected: $E_z(r = a)$. With $I_{\mathrm{C}} = j_{\mathrm{e}}\pi a^2$ and $I = I_{\mathrm{C}} - j_{\mathrm{e}}\pi r_{\mathrm{sat}}^2$ this results in [11]:

$$E_1(a) = \frac{\mu_0}{4\pi}\frac{\mathrm{d}I}{\mathrm{d}t}\ln\frac{1}{1-i} \quad \text{with } i = \frac{I}{I_{\mathrm{C}}}. \tag{4}$$

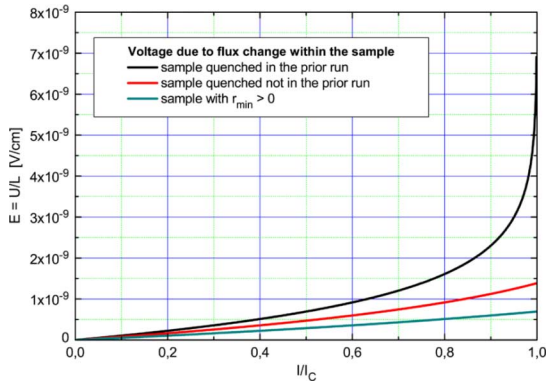

Fig. 2. Calculated voltage contribution due to flux change within the sample while ramping the transport current for a ramp rate of 1 A/s. Upper curve: Wire with a homogeneous distribution of the filaments over the cross sectional area in the first run or after quenching in the previous run according to equation (4). Middle curve: The same sample ramped near I_{C} in the previous run without quenching according to (6). Lower curve: Wire consisting of a ring of filaments with $r_{\min} = a/2$ according to (5).

The index '1' indicates that (4) is valid for the first measurement run of a sample.

Analogously, it can easily be shown that for a cylindric wire with an annular arrangement of the filaments, i.e. $0 < r_{\min} \leq r_{\mathrm{sat}}$, the electrical field in the first run is given by:

$$E_1^{\circ}(a) = \frac{\mu_0}{4\pi}\frac{\mathrm{d}I}{\mathrm{d}t}\ln\frac{1}{1 - i\frac{a^2 - r_{\min}^2}{a^2}} \quad \text{with } i = \frac{I}{I_{\mathrm{C}}}. \tag{5}$$

Where $r_{\min}$ is the position of the innermost rim of filaments.

For a second measurement following the first experimental run, the manner in which the first run was finished is crucial:

- *With quenching the sample.* When quenching the sample the flux profile in the sample is removed after the run. A subsequent run will reproduce the first $E(I)$-curve.
- *Without quenching the sample.* Ramping I near I_{C} and back to zero without quenching the sample retains a flux profile in the wire. Thus, in a subsequent run the flux entering the composite is less than in the first run. Consequently, the electrical field $E_n(a)$ generated in a subsequent current increase is smaller than in the first one. It can be shown [11], that for $r_{\min} = 0$ this field is given by

$$E_n(a) = \frac{\mu_0}{4\pi}\frac{\mathrm{d}I}{\mathrm{d}t}\ln\frac{2}{2-i}. \tag{6}$$

Fig. 2 overviews the different behavior of the voltage contributions due to flux change within the sample while ramping the current for the above discussed cases.

In addition to the internal self-field effect, other possible contributions to the measured voltage summarized in U_{other} could originate from the following causes:

- Voltage due to the current transfer from the copper terminals to the sample.
- Current transfer voltage due to current distribution among the superconducting filaments through the resistive matrix.
- Thermoelectric voltage.

The extent to which such causes contribute to the measured voltage will be discussed in the next section.

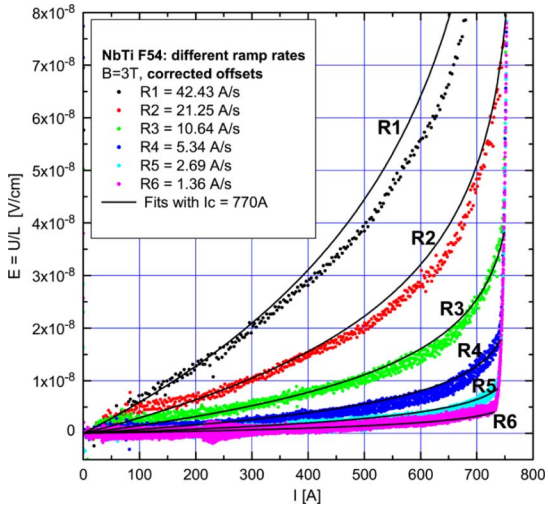

Fig. 3. Experimental data for the F54-sample for different ramp rates in an external field of 3 T after subtracting constant offset voltages. The solid lines are curves according to (4) with $I_{\mathrm{C}} = 770$ A.

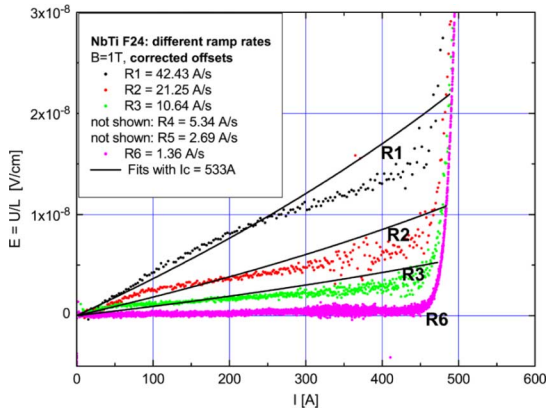

Fig. 4. Experimental data for the F24-sample for different ramp rates in an external field of 1 T after subtracting constant offset voltages. The solid lines are curves according to (5) with $I_{\mathrm{C}} = 533$ A. For the sake of clarity the data for $R4$ and $R5$ is not shown.

IV. Experimental and Discussion

A. Samples

To check the upgraded JUMBO facility and the implemented continuous measuring technique—among others—two one layer test coils with diameters of 90 mm of twisted round standard NbTi wire were manufactured: one coil made of a wire with 54 filaments (F54), another made of a wire with 24 filaments (F24). The wire diameters with insulation are 0.85 mm. Each coil consists of 16 turns. The voltage drop along the central two ($L_2 = 0.571$ m) and four ($L_1 = 1.142$ m) turns, respectively, was measured. To fix their positions, the superconducting wire and the (co-wound) voltage-taps were pasted over with Stycast, as already mentioned.

B. Results When Quenching the Samples

The experimental runs were performed in constant background fields at six different ramp rates $\mathrm{d}I/\mathrm{d}t$ from $R1 = 42.43$ A/s down to $R6 = 1.36$ A/s using the 10 T configuration of JUMBO. A waiting period of 2 minutes between each ramping allowed the recooling of the sample.

Fig. 3 shows the results for the F54-coil in an external field of 3 T when ramping the current up to the quench of the sample. As the curves for the two and four turns are identical only the latter are presented. To compare the curves, constant offset voltages were subtracted according to Section III-B, to ensure $E = 0$ at $I = 0$. With increasing ramp rate, a growing contribution to the measured voltage superimposing the signal caused by the superconducting transition occurs. The solid lines in Fig. 3 which describe the experimental data very well are 'fits' with (4) for $I_{\mathrm{C}} = 770$ A. It should be emphasized that (4) has no real free parameter as I_{C} is the critical current of the sample. I_{C} does indeed vary somewhat with the E-criterion, but is not free. In fact, 770 A is the critical current of the sample for $E = 1 \times 10^{-6}$ V/cm.

The results for the F24-coil after subtracting constant offset voltages are shown in Fig. 4. Again, the current was ramped up to the quench of the sample. In contrast to the F54-wire, the F24 consists of a ring-shaped arrangement of the filaments with $r_{\min} \approx 0.31$ mm. This geometry leads—according to (5) and Fig. 2—to a lower and non-divergent development of the voltage contribution due to the flux change within the sample. The experimental data is very well described with (5) using the critical current for the 10^{-6} V/cm-criterion of 533 A.

From these (and other not shown) measurements it can be concluded, that U_{other} is dominated by the voltage contribution due to the self-field effect within the sample. Other causes like current transfer or current distribution are of minor importance or negligible. This is due to our sample geometry with a current contact length at the copper terminals greater than one twist pitch and a length between the terminals and the first voltage tap greater than the current transfer length as discussed in [12]–[14].

C. Extrapolation: $\mathrm{d}I/\mathrm{d}t \to 0$

The question arises how the voltage contribution caused by the internal self-field effect can be eliminated to get the 'real' signal U_{SCT} originated by the superconducting transition. The simple subtraction of (4) is not possible because this equation is an approximation of reality that furthermore diverges for $I \to I_{\mathrm{C}}$. From (4)–(6) it follows that the internal self-field contribution is proportional to the ramp rate $\mathrm{d}I/\mathrm{d}t$. This can be proved e.g. for the experimental data of the F54-coil: If the data from Fig. 3 is divided by the used ramp rates, a single curve for the different runs is obtained (not shown). With S as the contribution due to the internal self-field effect for a ramp rate of 1 A/s and a rate independent U_{SCT}, it is possible to extrapolate the set of curves $U_m(I) = U_{\mathrm{SCT}}(I) + R_m S(I)$ measured for ramp rates $R_m > 0$ to $\mathrm{d}I/\mathrm{d}t \to 0$ to obtain a curve without the contribution of the inner self-field effect, as shown by the lowest curve in Fig. 5 (symbol ∘).

D. Influence of the Quench History

From the considerations in Section III-C, it follows that the quench history of the sample has an impact on the subsequent $U(I)$-measurement. Not quenching the sample retains a flux

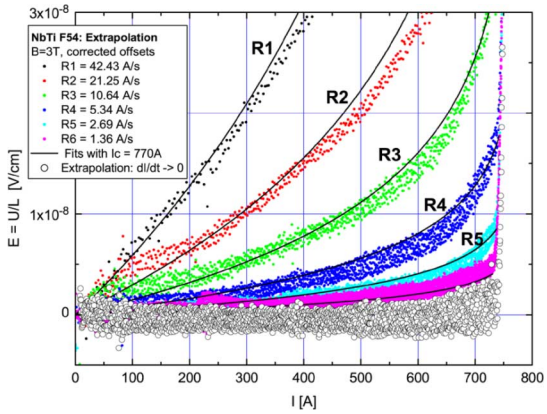

Fig. 5. Extrapolation of the data measured for the F54-coil with ramp rates >0 (see Fig. 3) to $\mathrm{d}I/\mathrm{d}t \rightarrow 0$ to obtain a curve without the contribution of the inner self-field effect as shown by the lowest curve ($\circ$).

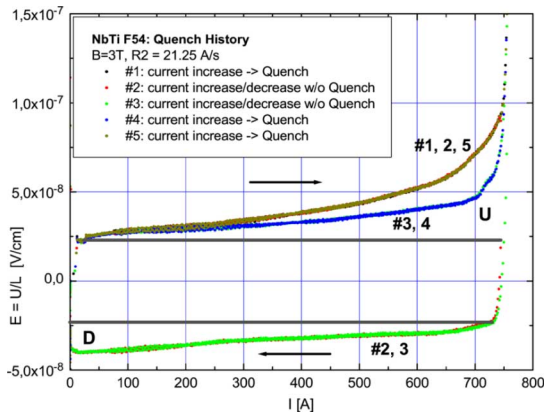

Fig. 6. Influence of the quench history on $U(I)$ for the F54-coil. For increasing current there exists a distinct splitting between the congruent runs {#1, 2, 5} in witch the sample was quenched in the prior run and the congruent runs {#3, 4} without quenching in the run before. When decreasing the current (curves {#2, 3}) there is no difference in $U(I)$ though the quench history of the sample was different in the two runs. Details in the text.

profile in the wire, reducing the contribution of the self-field effect in the following run. To investigate this issue, the following procedure with the F54-coil was performed:

- *Run #1:* Ramping the virgin sample up to quench. (The sample was quenched in the prior run.)
- *Run #2:* Ramping the sample without quenching near to I_C and back to $I = 0$.
- *Run #3:* Rerun of #2.
- *Run #4:* Ramping the sample up to quench.
- *Run #5:* Rerun of #4.

Fig. 6 shows the result of this procedure for a ramp rate of ± 21.25 A/s in a background field of 3 T. The bold horizontal lines positioned symmetrically to $E = 0$ indicate the constant offset voltage contributions U_IND for increasing and decreasing current, respectively, as discussed in Section III-B. The superimposed contributions above the upper (when ramping up; area $\mathbf{U}$) and below the lower line (when ramping down; area $\mathbf{D}$) are caused by the internal self-field effect. When increasing the current, there are two congruent families of curves: {#1, 2, 5} and {#3, 4}. In the first set, the sample was quenched in the prior run. In the second, there was no quench in the run before. This demonstrates that the quench history of a sample can have a distinct impact on ramped high resolution $U(I)$-measurements.

For decreasing current—curves {#2, 3}—there is no difference in $U(I)$, even though the quench history of the sample was different in the two runs. This means that the measured voltage is independent of the quench history when ramping down. This can be explained by the identical flux profile inside the sample—independent of the quench history—after ramping up near I_C, leading to the same $U(I)$ in the subsequent decreasing of the current.

V. Conclusion

The 15 T JUMBO facility was upgraded to perform ramped high resolution $U(I)$-measurements of superconductors. In detail, new measurement instrumentation was installed and the facility was revised to reduce the influence of perturbations. With the new setup a sampling rate of 14 Hz was achieved with a typical resolution of $\pm 1 \times 10^{-9}$ V/cm ($L \approx 100$ cm). First measurements with standard NbTi wire show that there exists a non-linear contribution to $U(I)$ due to the magnetic flux change within the sample while ramping the current. It was shown that this contribution depends on the quench history of the sample and the arrangement of the superconducting filaments within the specimen. By means of extrapolation of the data measured for ramp rates >0 to $\mathrm{d}I/\mathrm{d}t \rightarrow 0$ it was possible to eliminate the contribution caused by the inner self-field effect.

References

[1] A. Rimikis, F. Hornung, and Th. Schneider, "High field magnet facilities and projects at the Forschungszentrum Karlsruhe," *IEEE Trans. Appl. Supercond.*, vol. 10, pp. 1542–1545, 2000.

[2] H. Leibrock, F. Hornung, M. Kläser, H. Müller, and Th. Schneider, "Error analysis of $E(I)$-measurements on NbTi-superconductors," *Physica C*, vol. 401, pp. 255–259, 2004.

[3] R. Kimmich, F. Hornung, A. Rimikis, Th. Schneider, and P. J. Lee, "Microstructure and current-voltage characteristics of bronze processed Niobium Tin composites," *IEEE Trans. Appl. Supercond.*, vol. 11, pp. 3675–3678, 2001.

[4] F. Hornung, A. Rimikis, R. Kimmich, and Th. Schneider, "Investigation of Bi-HTS wires for high field insert coils," *IEEE Trans. Appl. Supercond.*, vol. 11, pp. 2304–2307, 2001.

[5] F. Hornung, M. Kläser, H. Leibrock, H. Müller, and Th. Schneider, "Suitability of Bi-HTS wires for high field magnets," *Physica C*, vol. 401, pp. 218–221, 2004.

[6] F. Hornung, M. Kläser, and Th. Schneider, "Usage of Bi-HTS In high field magnets," *IEEE Trans. Appl. Supercond.*, vol. 14, pp. 1102–1105, 2004.

[7] M. Beckenbach, F. Hornung, M. Kläser, P. Leys, B. Lott, and Th. Schneider, "Manufacture and test of a 5 T Bi-2223 insert coil," *IEEE Trans. Appl. Supercond.*, vol. 15, pp. 1484–1487, 2005.

[8] H. Müller, F. Hornung, A. Rimikis, and Th. Schneider, "Critical current distribution in composite superconductors," *IEEE Trans. Appl. Supercond.*, vol. 17, pp. 3757–3760, 2007.

[9] F. Hornung, M. Kläser, and T. Schneider, "Degradation of Bi-2223 tape after cooling with superfluid Helium," *IEEE Trans. Appl. Supercond.*, vol. 17, pp. 3117–3120, 2007.

[10] M. N. Wilson, *Superonducting Magnets*. Oxford: Clarendon Press, 1983.

[11] J. L. Duchateau, B. Turck, L. Krempasky, and M. Polak, "The self-field effect in twisted superconducting composites," *Cryogenics*, vol. 16, pp. 97–102, 1976.

[12] J. W. Ekin, "Current transfer in multifilamentary superconductors. I. Theory," *J. Appl. Phys.*, vol. 49, pp. 3406–3409, 1978.

[13] J. W. Ekin, A. F. Clark, and J. C. Ho, "Current transfer in multifilamentary superconductors. II. Experimental results," *J. Appl. Phys.*, vol. 49, pp. 3410–3412, 1978.

[14] L. Dresner, "Distribution of current among the filaments of a multifilamentary superconductor close-to the input leads," *Cryogenics*, vol. 18, pp. 285–288, 1978.